

## Electronic Supplementary Information for

### Self-Assembly of Two Ring-shape Hexanuclear Mo(VI) Clusters

Lu Yang,<sup>a</sup> Zhen Zhou,<sup>a</sup> Pengtao Ma,<sup>a</sup> Jingping Wang,<sup>\*a</sup> and Jingyang Niu<sup>\* a,b</sup>

<sup>a</sup>Henan Key Laboratory of Polyoxometalate, Institute of Molecular and Crystal Engineering, College of Chemistry and Chemical Engineering, Henan University

Kaifeng, Henan 475004, China

Fax: (+86) 378-3886876, E-mail: jpwang@henu.edu.cn, jyniu@henu.edu.cn

<sup>b</sup>State Key Laboratory of Coordination Chemistry, Nanjing, Jiangsu, China

**Figure S1.** IR spectra of compounds **1** and **2**

**Figure S2.** Comparison of the simulated (in red) and experimental XRPD patterns (in blue) of **1**.

**Figure S3.** Comparison of the simulated (in red) and experimental XRPD patterns (in blue) of **2**.

**Figure S4.** <sup>31</sup>P spectrum of the ATMP ligand dissolved in D<sub>2</sub>O at room temperature.

**Figure S5.** Plot of the reduced magnetization ( $M/N\mu_B$ ) vs  $H/T$  at the indicated applied fields.

**Figure S6.** Charge distribution of O atoms in the fragment of **1**.

**Figure S7.** Charge distribution of O atoms in the fragment of **2**.

**Figure S8.** The 1D chain structure of **1** along  $a$  axis.

**Figure S9.** The 1D chain structure of **2** along  $a$  axis.

**Table S1.** The bond valence sum calculations of all the oxygen atoms on POM fragments in **1**.

**Table S2.** The bond valence sum calculations of all the oxygen atoms on POM fragments in **2**.

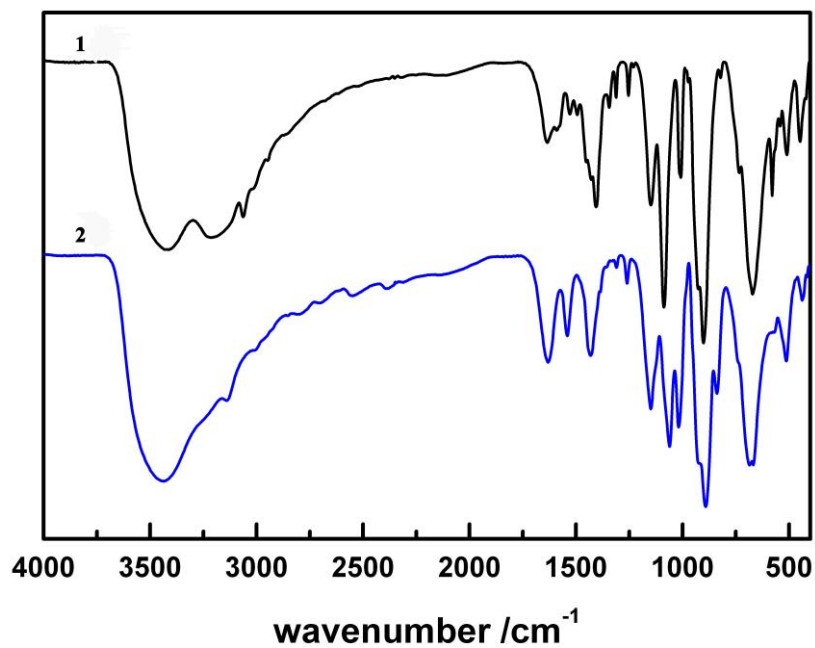


Figure S1. IR spectra of compounds 1 and 2

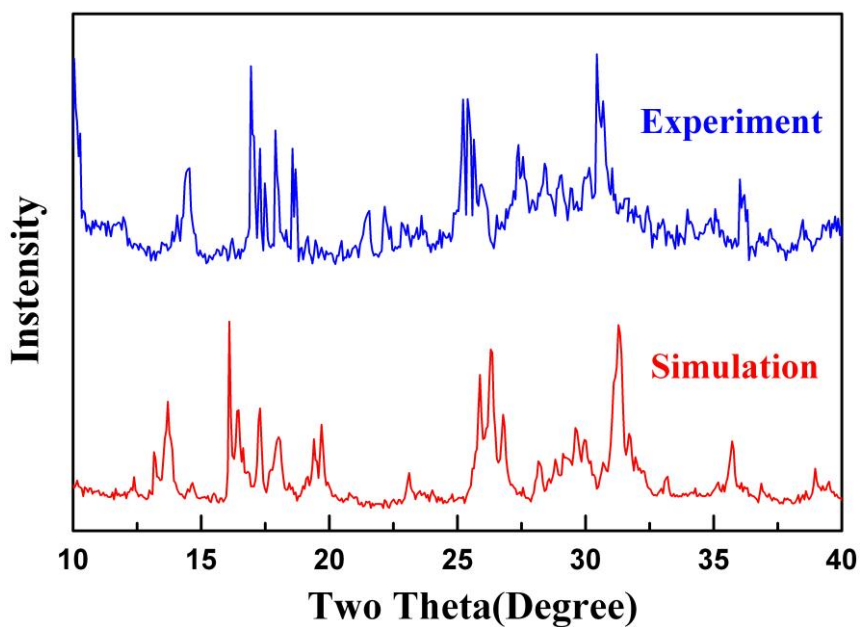
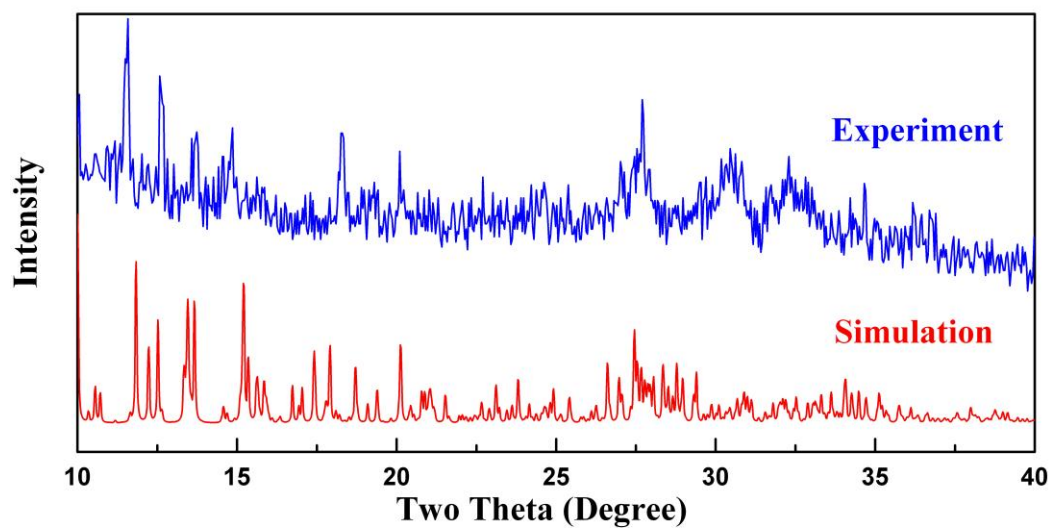
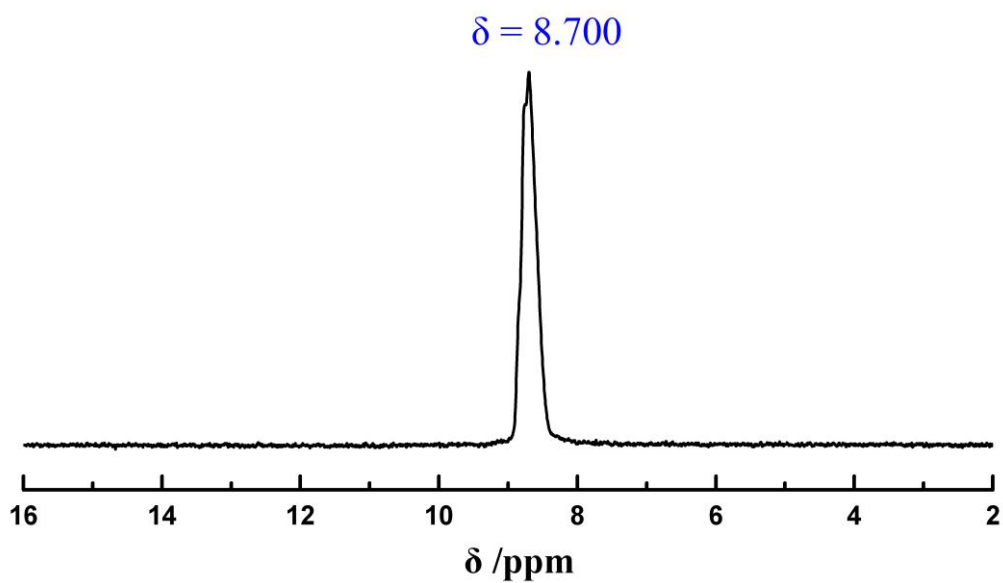


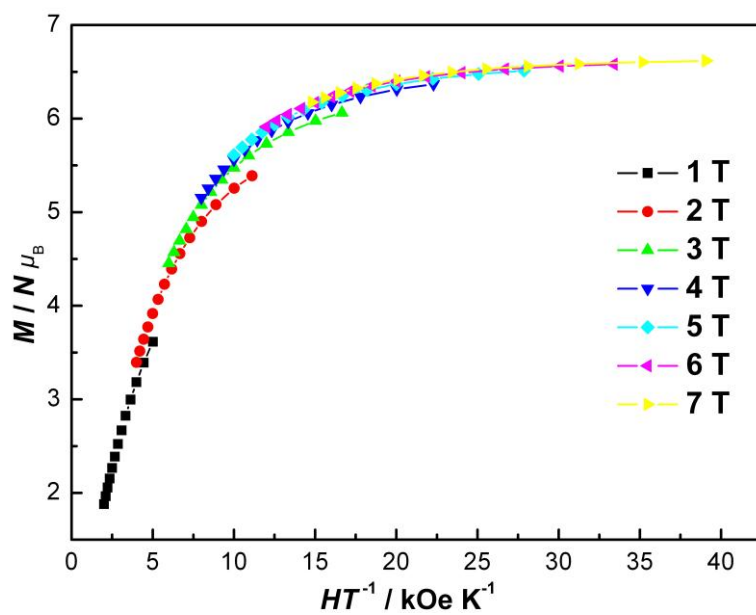
Figure S2. Comparison of the simulated (in red) and experimental XRPD patterns (in blue) of 1. Their peak positions are in good agreement with each other, indicating the phase purity of the products. The differences in intensity may be due to the preferred orientation of the powder samples.



**Figure S3.** Comparison of the simulated (in red) and experimental XRPD patterns (in blue) of **2**.



**Figure S4.** <sup>31</sup>P spectrum of the ATMP ligand dissolved in D<sub>2</sub>O at room temperature.





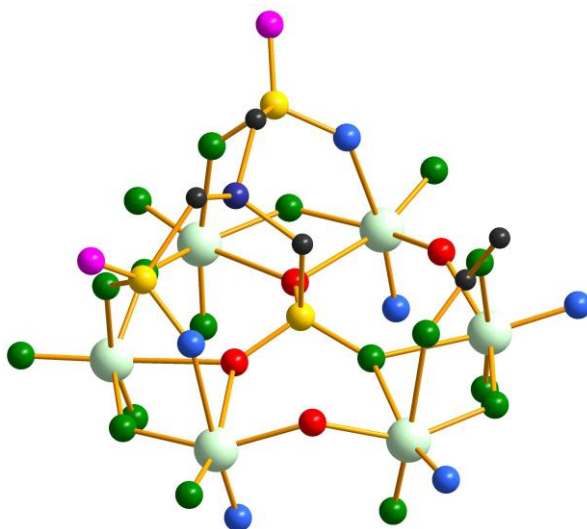


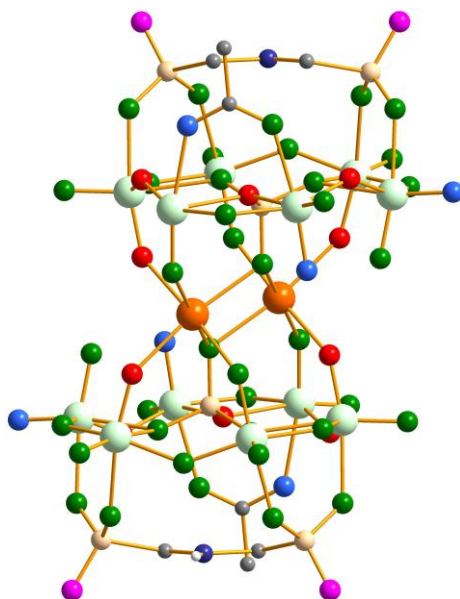
**Figure S5.** Plot of the reduced magnetization ( $M/N\mu_B$ ) vs  $H/T$  at the indicated applied fields.



**Figure S6.** Charge distribution of O atoms in the fragment of **1**. Oxygen atoms with different bond valence sums are represented by different colors. H atoms, Na<sup>+</sup> and lattice water molecules are omitted for clarity.





**Table S1.** The bond valence sum calculations of all the oxygen atoms on POM fragments in **1**.

Oxygen	Band valence sum range	Number	Oxygen	Band valence sum range	Number
	-2.00 ~ -1.91	4		-1.90 ~ -1.71	17
	-1.70 ~ -1.51	6		-1.50 ~ -1.31	2



**Figure S7.** Charge distribution of O atoms in the fragment of **2**. Oxygen atoms with different bond valence sums are represented by different colors. H atoms, Na<sup>+</sup> and lattice water molecules are omitted for clarity.

**Table S2.** The bond valence sum calculations of all the oxygen atoms on POM fragments in **2**.

Oxygen	Band valence sum range	Number	Oxygen	Band valence sum range	Number
	-2.00 ~ -1.91	10		-1.90 ~ -1.71	40
	-1.70 ~ -1.51	6		-1.50 ~ -1.31	4

There are some protons are needed to compensate the negative charges of the polyanion in **1** and **2** due to the charge-balance consideration. On the basis of valence sum ( $\Sigma_s$ ) calculations, the multiply protonated fragments in both compounds are reasonable. Compounds **1** and **2** were synthesized in the acidity condition and might be prone to be protonated. In generally, the multiply protons cannot be located in polyoxometalate fragments by X-ray diffraction, and they are usually assigned to be delocalized on the whole polyoxoanion only for balancing the high negative charges of the polyoxoanion at different synthetic conditions, which is common in polyoxometalate chemistry and has been reported in many literatures, such as  $[\text{H}_4\text{P}_2\text{W}_{12}\text{Fe}_9\text{O}_{56}(\text{OAc})_7]^{6-}$ <sup>[S1]</sup>,  $[\text{H}_3\text{W}_{12}\text{O}_{40}]^{5-}$ <sup>[S2]</sup> and  $[\text{H}_6\text{Ni}_{20}\text{P}_4\text{W}_{34}(\text{OH})_4\text{O}_{136}(\text{enMe})_8(\text{H}_2\text{O})_6]^{6-}$ <sup>[S3]</sup>. For **1**, there are four O atoms with their  $\Sigma_s$  in the range of -2.00 ~ -2.91, seventeen O atoms with their  $\Sigma_s$  in the range of -1.90 ~ -1.71, six O atoms with their  $\Sigma_s$  in the range of -1.70 ~ -1.51 and two O atoms with their  $\Sigma_s$  in the range of -1.50 ~ -1.31. For **2**, there are ten O atoms with their  $\Sigma_s$  in the range of -2.00 ~ -2.91, forty O atoms with their  $\Sigma_s$  in the range of -1.90 ~ -1.71, six O atoms with their  $\Sigma_s$  in the range of -1.70 ~ -1.51 and four O atoms with their  $\Sigma_s$  in the range of -1.50 ~ -1.31. From these results of bond valence sum ( $\Sigma_s$ ) calculations, firstly, we can distinguish the different oxygen states of -2 or -1 for O atoms and also confirm the locations of the additional protons in **1**, which are likely to be considered as the average bond valence sums of these O

atoms (represented by green and blue), especially the six O atoms with their  $\Sigma_s$  in the range of  $-1.70 \sim -1.51$  according to the literatures.<sup>[S3]</sup>

**Reference:**

[S1] B. Godin, Y. G. Chen, J. Vaissermann, L. Ruhlmann, M. Verdaguer, P. Gouzerh, *Angew. Chem. Int. Ed.*, 2005, **44**, 3072.

[S2] C. Streb, C. Ritchie, D. L. Long, P. Kögerler, L. Cronin, *Angew. Chem. Int. Ed.*, 2007, **46**, 7579.

[S3] S. T. Zheng, J. Zhang, J. M. Clemente-Juan, D. Q. Yuan, G. Y. Yang, *Angew. Chem. Int. Ed.*, 2009, **48**, 7176.

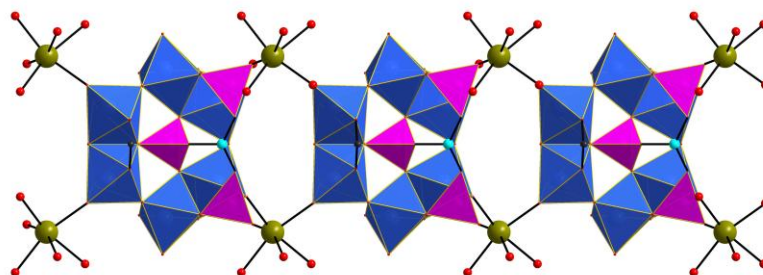


**Figure S8.** The 1D chain structure of **1** along *a* axis.

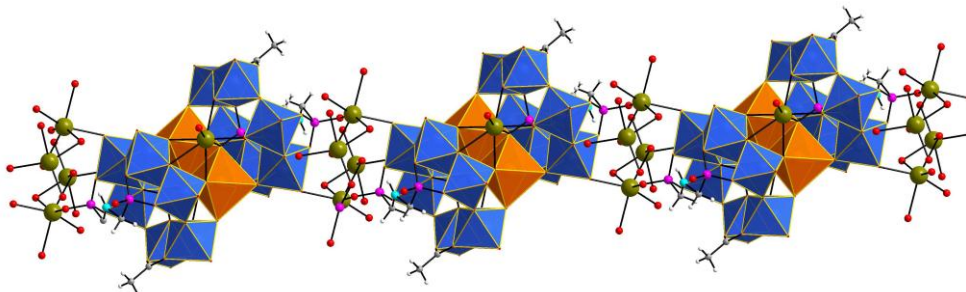


**Figure S9.** The 1D chain structure of **2** along *a* axis.